Effect of nanoparticle scattering on thermoelectric power factor

Mona Zebarjadi,[1,a)] Keivan Esfarjani,[1,2] Ali Shakouri,[1] Je-Hyeong Bahk,[3] Zhixi Bian,[1] Gehong Zeng,[3] John Bowers,[3] Hong Lu,[4] Joshua Zide,[5] and Art Gossard[4]

[1]*Department of Electrical Engineering, University of California, Santa Cruz, California 95064, USA*
[2]*Department of Physics, University of California, Santa Cruz, California 95064, USA*
[3]*Electrical and Computer Engineering Department, University of California Santa Barbara, California 93106, USA*
[4]*Department of Materials, University of California Santa Barbara, California 93106, USA*
[5]*Department of Electrical and Computer Engineering, University of Delaware, Newark, Delaware 19716, USA*

The effect of nanoparticles on the thermoelectric power factor is investigated using the relaxation time approximation. The partial-wave technique is used for calculating the nanoparticle scattering cross section exactly. We validate our model by comparing its results to the experimental data obtained for ErAs:InGaAlAs samples. We use the theory to maximize the power factor with respect to nanoparticle and electron concentrations as well as the barrier height. We found that at the *optimum* of the power factor, the electron concentration is usually higher in the sample with nanoparticles, implying that Seebeck is usually unchanged and conductivity is increased. © *2009 American Institute of Physics*. [DOI: 10.1063/1.3132057]

In recent years, along with advancement in material synthesis, it has been possible to embed nanoparticles with controlled size in bulk materials. The advantage of incorporating nanoparticles inside thermoelectric materials is to reduce the lattice thermal conductivity[1] and enhance the Seebeck coefficient due to electron energy filtering.[2] Depending on their radius, volume fraction, and band offset, a nanoparticle-doped sample can either suppress or enhance the electrical conductivity in comparison with the doped bulk sample. Generally, enhancement of the electrical conductivity is accompanied by suppression of the Seebeck coefficient and vice versa. Therefore, careful design is needed to enhance the thermoelectric power factor ($P = S^2\sigma$: Seebeck coefficient squared times electrical conductivity).

Recently, Faleev and Leonard[3] suggested an enhancement of the thermoelectric power factor in semiconductors with metallic nanoinclusions at high doping concentrations. They used the partial wave (PW) technique to calculate the scattering rates from nanoparticles. However, the results are based on Eq. (35) in their paper, which is incorrect. In contrast to their prediction, we find that there is a big difference between a nanoparticle well potential and a barrier potential.

The PW method is used to calculate the scattering cross section from a spherically symmetric potential. The result for the total cross section (σ) is well known.[4] For the momentum scattering cross section (σ_m), we find the expression shown in Eq. (2),

$$\sigma(\theta) = \frac{1}{k^2}\left|\sum_{l=0}^{\infty}(2l+1)e^{i\delta_l}\sin\delta_l P_l(\cos\theta)\right|^2, \quad (1)$$

$$\sigma_m = \frac{4\pi}{k^2}\left[\sum_{l=0}^{\infty}(2l+1)\sin^2\delta_l - \sum_{l=0}^{\infty}2l\cos(\delta_l-\delta_{l-1})\sin\delta_l\sin\delta_{l-1}\right], \quad (2)$$

$$\tan\delta_l = \frac{kj_l'(ka)-y_l j_l(ka)}{kn_l'(ka)-y_l n_l(ka)} \quad y_l = \left.\frac{\varphi'}{\varphi}\right|_{r=a}. \quad (3)$$

Here, δ_l is called the phase shift of the lth PW (l being the angular momentum quantum number), φ is the wave function of the electron inside the nanoparticle, k is the wave vector and a is the particle radius. P_l is the Legendre function. j_l and n_l are the spherical Bessel functions of the first and second kind, respectively. For a known potential shape and a given energy, the solution of the Schrödinger equation can be found numerically inside the nanoparticle using the shooting method.[5] Then y_l is calculated by matching the
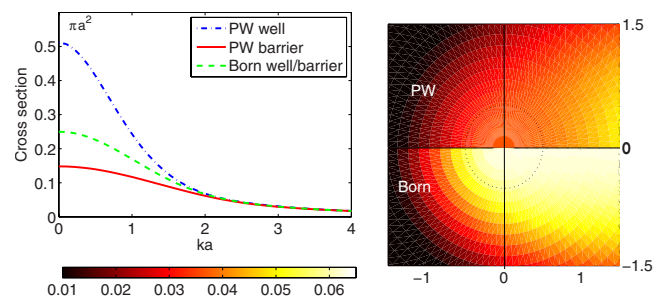

FIG. 1. (Color online) Comparison between the Born approximation and the partial-wave method. Left: Scattering cross section in units of πa^2 for the partial-wave and Born approaches. The barrier/well energy scale ($2Va^2$) here is 0.75. Right: differential scattering cross section as a function of electron momentum (horizontal axis is in the direction of the incident wave and the vertical axis is in the transverse direction). We assumed a potential barrier. The differential scattering cross section is shown for the PW method (top right) and for the Born approximation (bottom right).

a)Electronic mail: mona@soe.ucsc.edu.

wave function at the boundary between the nanoparticle and the host material.

For modeling a realistic material, we need to include other scattering mechanisms such as phonons and impurities in the formalism. We use the variational method which was developed by Howarth and Sondheimer[6] and later expanded to the case of nonparabolic band structure and screened phonons by Ehrenreich[7] to include the inelastic mechanism of the electron-polar optical phonon scattering. Electrons are assumed to scatter elastically from the other scatterers. Thermoelectric properties can be obtained by using the linear response theory and by integrating the differential conductivity over energy,

$$S = \frac{1}{eT} \left[\frac{\int \nu^2 (E - \mu) \tau_f(E) \text{DOS}(E) \frac{\partial f}{\partial E} dE}{\int \nu^2 \tau_f(E) \text{DOS}(E) \frac{\partial f}{\partial E} dE} \right]. \quad (4)$$

$$\frac{1}{\rho} = -\frac{2e^2}{3m^*} \int E \tau_f(E) Dos(E) \frac{\partial f}{\partial E} dE. \quad (5)$$

Here, S is the Seebeck coefficient, ρ is the resistivity, ν is the group velocity, μ is the chemical potential, τ_f is the distribution function relaxation time, $\text{DOS}(E)$ is the density of states at energy E and $f(E)$ is the Fermi–Dirac distribution function. Material properties, such as effective mass, nonparabolic parameter, dielectric constant, phonon energy, sound velocity, etc., are set by interpolating experimental parameters of InGaAs and InAlAs.[8]

In Fig. 1 we have compared the scattering cross sections resulting from the Born approximation[4] and the PW method. The Born approximation is based on the perturbation theory and therefore it has the intrinsic assumption that the potential of the scatterer is weak. This approximation works well for energies, which are several times the barrier height.

In the Born approximation, at small angles low-energy electrons' partial scattering cross section is the same as that of the high-energy ones. Using the PW method, scattering cross section increases with energy in the forward direction (see Fig. 1 right: follow the theta=0 line). Therefore, nanoparticles affect low-energy electrons more than the high-energy ones, which is a kind of electron filtering. However, we noticed that this difference is not much and it does not lead to a significant increase in the Seebeck. This is because the system is three-dimensional. Low-energy electrons are more scattered but they still contribute to the total electrical conductivity.

To verify the effect of nanoparticles on the thermoelectric transport we studied two samples. These samples are InGaAlAs with 20% Al concentration grown on lattice-matched InP substrate. Since the InP substrate becomes conductive at above 600 K, and affects the conductivity and Seebeck measurements at the high temperatures, the InP substrate had to be removed. Then the samples were bonded on to Sapphire plates. One sample was doped with 2×10^{18} cm^{-3} concentration of silicon. To the other sample, 0.3% Erbium was added during growth. In this sample, ErAs nanoparticles are formed coherently inside the bulk matrix with sizes ranging from 2 to 3 nm.[9] Hall measurement data indicates a carrier concentration of 7×10^{17} cm^{-3} at 300 K
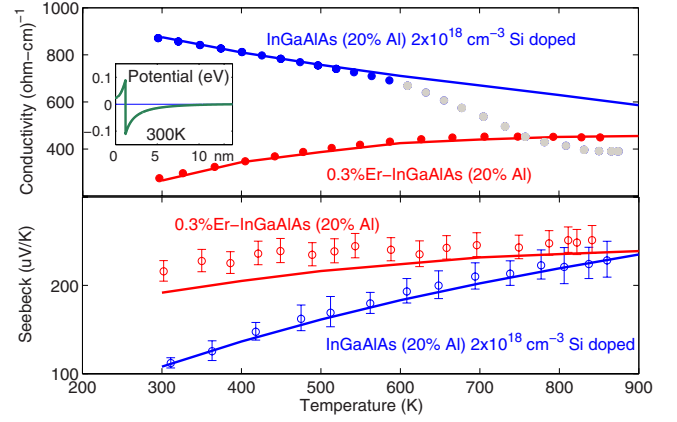

FIG. 2. (Color online) Comparison of the theory with experiment: Circles are experimental data and solid lines are theoretical prediction. Electrical conductivities were fitted (using alloy potential for the doped sample and using a_0 and the Schottky barrier height for the nanoparticle sample as fitting parameters), and the Seebeck coefficients were predicted. Experimental electrical conductivity data above 600 K for the sample without nanoparticles were not reproducible; those are shown with gray circles. Potential profile of single nanoparticles at 300 K is plotted inside the top figure.

and a carrier concentration of 3×10^{18} cm^{-3} at 800 K for the latter sample. In-plane Seebeck and conductivity were measured and reported in Fig. 2.

To explain the data of the Si-doped sample we calculated acoustic and polar optical phonons as well as ionized impurity, alloy, electron-electron and electron-hole scatterings. The conductivity data of this sample is fitted using the strength of the alloy potential as a single fitting parameter. The alloy potential was found to be 0.33 eV. The Seebeck coefficient was then predicted. The theory is in good agreement with the experiment in the range of 300–600 K [Fig. 2(b)]. Experimentally, we observed sudden drop of conductivity at above 600 K [highlighted in the blue dot curve of Fig. 2(a)]. That is believed to be due to sample degradation, as we could not reproduce the room temperature experimental data after the high temperature measurements. This is probably due to insufficient sample passivation and degassing at high temperatures.

Nanoparticle scattering rate is then added to the other rates to explain the data of the sample with nanoparticles. We assumed a uniform positive background density inside the nanoparticle and used the Thomas–Fermi model of screening to obtain the potential profile by solving the Poisson equation.

$$\rho(r) = \frac{z}{4/3 \pi a_0^3} \quad 0 < r < a_0,$$

$$V(q) = \frac{4\pi}{q^2 + \lambda^2} \rho(q),$$

$$V(r) = \int_{-\infty}^{\infty} V(q) e^{iq.r} \frac{d^3q}{(2\pi)^3} + E_{\text{Schottky}} \theta(r - a), \quad (6)$$

where θ is the step function, $1/\lambda$ is the Thomas–Fermi screening length, z is the number of electrons per nanoparticle contributing to the conduction band, a is the nanoparticle radius which is known from the TEM imaging to be 1.2 nm on the average, and a_0 is the length over which positive charges are assumed to distribute uniformly. This length
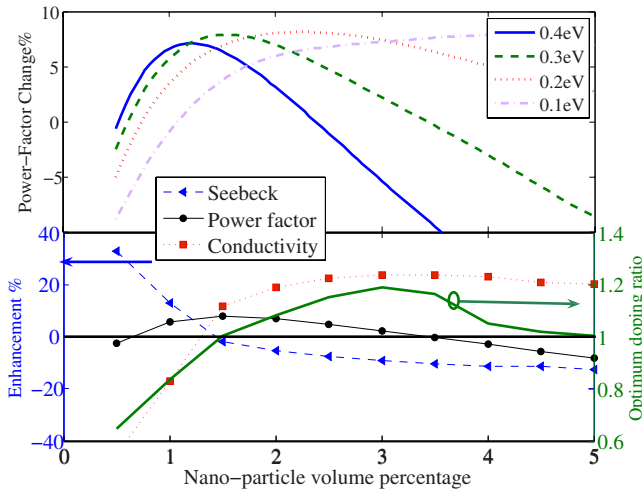
FIG. 3. (Color online) (a) Enhancement of the power factor of the nanoparticle sample with respect to that of the Si-doped sample. This plot was obtained by maximizing the power factor versus carrier concentration at each fixed nanoparticle concentration and Schottky barrier height. Maximum power factor of the bulk material with dopants instead of nanoparticles is taken as the reference point (b): enhancement of the power factor for the barrier height of 0.3 eV. The corresponding change in the Seebeck and the conductivity along with the ratio of the optimum electron concentration of the samples with embedded nanoparticle to that of the bulk material were also plotted.

(about 1 nm) and the height of the Schottky barrier between the host matrix and the nanoparticle (about 0.2 eV) are used to fit the conductivity data. Total number of carrier concentration is set from the Hall data. Fitting results of the electrical conductivity with $E_{Schottky}$ and a_0 are shown in Fig. 2(a). There again the Seebeck coefficient is predicted with no extra fitting. One can note a systematic underestimation of the Seebeck coefficient [Fig. 2(b)]. The difference may come from the fact that the real potential of the nanoparticles is not known and that we have a simplified model of the potential distribution around nanoparticles. In the case of the sample with nanoparticles, we did not notice any degradation at high temperatures and the data at room temperature was reproducible.

We then used these fitted and all the rest of materials parameters and optimized the thermoelectric properties of the nanocomposite material versus carrier concentration, nanoparticle concentration and Schottky barrier height. At a fixed nanoparticle concentration, the power factor is maximized versus carrier concentration. Then the maxima are plotted versus the nanoparticle concentration (Fig. 3). Maximum power factor of the bulk material (with dopants instead of nanoparticles) is used as the reference point when the percentage of enhancement is reported. At room temperature and at 800 K, we have observed that an enhancement in the thermoelectric power factor up to 8% and 5%, respectively, can be obtained.

Figure 3(a) shows the plot of power factor versus nanoparticle volume fraction for four different barrier heights. The peak value of the maximum power versus nanoparticle volume fraction (~8% in this case) does not change much with the barrier height, but its position does. It seems that the optimum power factor is always obtained for the same value of the average barrier height per volume, which is roughly proportional to the barrier height multiplied by the nanopar-

ticle concentration. That is, if we double the barrier height, the optimum volume fraction is reduced by a factor of 2.

The optimum value of electron concentration of samples with high volume fraction of nanoparticles (more than 1.5%) was found to be larger than the samples without nanoparticles. Therefore as Fig. 3(b) shows when the power factor is maximized, the Seebeck coefficient does not change much but the electrical conductivity is increased. Increase in the electrical conductivity also comes from the fact that because of its size a nanoparticle can contribute more electrons to the conduction band compared to a dopant. Then for the same electron concentration, number of scatterers (nanoparticles compared to dopants) can be smaller, leading to an increase in the mobility.

In summary, the Born approximation cannot quantitatively predict the transport properties of a bulk matrix with embedded nanoparticles when the nanoparticle barriers are larger than the energy scales of the problem (Fermi level, $k_B T$, etc.). Using the PW method, scattering increases in the forward direction as the energy increases but Born approximation predicts that forward scattering is independent of the electron energy. Nanoparticles can increase or decrease the thermoelectric power factor. This depends on their concentration, their potential profile inside the bulk matrix and also on the position of the Fermi level. Using our model, we could explain the measured Seebeck coefficient and electrical conductivity of bulk InGaAlAs as well as those of a InGaAlAs sample with 0.3% volume concentration of ErAs nanoparticles. We optimized the composition of the nanoparticle sample and showed that at room temperature, the maximum enhancement in power factor is around eight percent. For the adopted class of nanoparticle potential (repulsive core coated with a damped attractive layer), the increase in the thermoelectric power factor comes form the enhancement of the electrical conductivity rather than the enhancement of the Seebeck coefficient. A proper engineering of the nanoparticle potential can however lead to both Seebeck and electrical conductivity enhancement. This and the effect of multiple scatterings on the thermoelectric properties of nanoparticle samples at higher concentrations are the subject of a future publication.

[1] W. Kim, S. L. Singer, A. Majumdar, D. Vashaee, Z. X. Bian, A. Shakouri, G. H. Zeng, J. E. Bowers, J. M. O. Zide, and A. C. Gossard, Appl. Phys. Lett. **88**, 242107 (2006).
[2] G. H. Zeng, J. M. O. Zide, W. Kim, J. E. Bowers, A. C. Gossard, Z. X. Bian, Y. Zhang, A. Shakouri, S. L. Singer, and A. Majumdar, J. Appl. Phys. **101**, 034502 (2007).
[3] S. V. Faleev and F. Leonard, Phys. Rev. B **77**, 214304 (2008).
[4] L. I. Schiff, *Quantum Mechanics* (McGraw-Hill, New York, 1949).
[5] J. Stoer and R. Bulirsch, *Introduction to Numerical Analysis* (Springer, New York, 1980).
[6] D. J. Howarth and E. H. Sondheimer, Proc. R. Soc. London, Ser. A, **219**, 53 (1953).
[7] H. Ehrenreich, J. Phys. Chem. Solids **2**, 131 (1957).
[8] Ioffe Physico-Technical Institute, http://www.ioffe.rssi.ru/SVA/; Landolt-Börnstein online database, http://www.springer.com/west/home/laboe?SGWID4-10113-0-0-0.
[9] D. O. Klenov, J. M. O. Zide, J. M. LeBeau, A. C. Gossard, and S. Stemmer, Appl. Phys. Lett. **90**, 121917 (2007).